^{18}F-FDOPA PET and PET/CT Accurately Localize Pheochromocytomas

Farzin Imani[1], Vatche G. Agopian[2], Martin S. Auerbach[1], Martin A. Walter[1], Firoozeh Imani[1], Matthias R. Benz[1], Rebecca A. Dumont[1], Chi Kien Lai[3], Johannes G. Czernin[1], and Michael W. Yeh[2]

[1]Ahmanson Biological Imaging Division, Department of Molecular and Medical Pharmacology, David Geffen School of Medicine at UCLA, Los Angeles, California; [2]Endocrine Surgical Unit, Department of Surgery, David Geffen School of Medicine at UCLA, Los Angeles, California; and [3]Department of Pathology and Laboratory Medicine, David Geffen School of Medicine at UCLA, Los Angeles, California

Successful treatment of pheochromocytoma requires accurate diagnosis and localization of tumors. Herein, we investigated the accuracy of PET using 3,4-dihydroxy-6-^{18}F-fluoro-phenylalanine (^{18}F-FDOPA), an amino acid transporter substrate, as an independent marker for detection of benign and malignant pheochromocytomas. **Methods:** The study comprised 25 consecutive patients (9 men, 16 women) whose median age was 51 y (range, 25–68 y), with known or suspected pheochromocytoma. Eleven patients underwent standardized ^{18}F-FDOPA PET and 14 patients underwent ^{18}F-FDOPA PET/CT studies, with a median of 511 MBq of ^{18}F-FDOPA (range, 206–625 MBq). Two readers, unaware of the reports of other imaging studies and clinical data, analyzed all scans visually and quantitatively (maximum standardized uptake value [SUVmax] and maximum transverse diameter). Histology and long-term clinical follow-up served as the gold standard. Correlation between SUVmax of tumors and biochemical markers was evaluated. SUVmax of the benign and malignant tumors was compared. **Results:** Seventeen patients underwent surgery. Histology confirmed pheochromocytoma or paraganglioma in 11 cases (8 adrenal, including 2 malignant tumors, and 3 extraadrenal, including 1 malignant tumor). The diagnosis of pheochromocytoma was established by follow-up in 2 additional patients (1 adrenal and 1 unknown location) and ruled out in 6 patients. Visual analysis detected and localized pheochromocytoma in 11 of 13 patients without false-positive results (sensitivity, 84.6%; specificity, 100%; accuracy, 92%). These lesions had an SUVmax of 2.3–34.9 (median, 8.3). Evaluation of the false-negative cases revealed a 13 × 5 mm lesion with an SUVmax of 1.96 in 1 case; no lesion was localized in the second case using multiple additional modalities. Spearman nonparametric analysis did not show statistically significant correlation between SUVmax of the tumors and biochemical markers. The Mann–Whitney nonparametric test did not demonstrate a statistically significant difference between the SUVmax of ^{18}F-FDOPA in malignant and benign tumors. **Conclusion:** ^{18}F-FDOPA PET and PET/CT are highly sensitive and specific tools that can provide additional independent information for diagnosis and localization of benign and malignant pheochromocytomas.

Received Sep. 23, 2008; revision accepted Dec. 10, 2008.
For correspondence or reprints contact: Farzin Imani, P.O. Box 24783, Los Angeles, CA, 90024.
E-mail: fimani@nucmed.com
Guest Editor: R. Ed Coleman, Duke University Medical Center

Key Words: ^{18}F-FDOPA PET; ^{18}F-FDOPA PET/CT; pheochromocytoma; paraganglioma; adrenal gland tumor

J Nucl Med 2009; 50:513–519
DOI: 10.2967/jnumed.108.058396

The anatomic imaging modalities CT and MRI are currently the main imaging techniques used for localizing pheochromocytomas. Although the sensitivity of localizing tumors confined to the adrenals can reach 95% for CT or MRI (*1*), these modalities have limited specificity (*2*) because of metastatic and extraadrenal tumors. New imaging methods with higher specificity can play a crucial role in the diagnosis and localization of tumors.

PET with ^{18}F-FDG, the main radiopharmaceutical imaging agent in oncology, has been shown to be limited because of the lack of specificity for neuroendocrine tumors (*3,4*), which are generally well differentiated and slow growing. ^{11}C-epinephrine and ^{11}C-hydroxyephedrine catecholamine analogs developed for studying the sympathetic nervous system have provided good results (*4–6*); however, their widespread clinical use is limited by the short physical half-life of ^{11}C, which limits the acquisition time and requires on-site cyclotron production. ^{18}F-labeled radiopharmaceuticals with longer half-lives and active uptake in neuroendocrine cells can eliminate these limitations. ^{18}F-fluorodopamine has recently been evaluated for detection of pheochromocytoma and has provided improved results (*7–9*). In this study, we evaluated 3,4-dihydroxy-6-^{18}F-fluoro-phenylalanine (^{18}F-FDOPA). A review of the literature revealed a few studies concentrating on ^{18}F-FDOPA PET of pheochromocytomas (Table 1) (*10–13*). The aims of this study were to evaluate the accuracy of PET and PET/CT with ^{18}F-FDOPA in detecting and localizing pheochromocytomas and assess the relationship between biochemical markers and tracer uptake (in the expectation that a better understanding of this relationship could improve the selection of patients for specific imaging studies). In addition, another aim of this study was to compare ^{18}F-FDOPA uptake in benign and malignant pheochromocytomas.

TABLE 1. Review of Studies Concentrating on ^{18}F-FDOPA PET of Pheochromocytomas

Author	Date	Total subjects (*n*)	Histology	Gold standard	Sensitivity	Specificity
Hoegerle et al. (*10*)	2002	14	8	Histology and MRI	100%	100%
Timmers et al. (*11*)	2007	11	N/A	CT and MRI	66.70%*	N/A
Taieb et al. (*12*)	2008	9	N/A	Clinical history and CT, MRI, ^{131}I-MIBG, ^{111}In-DTPA-pentetreotide	100%	N/A

*Sensitivity for body regions with carbidopa.

MATERIALS AND METHODS

Inclusion Criteria

We included all adult patients with suspected pheochromocytoma (based on clinical symptoms, biochemical results, or previous morphologic imaging studies) who had been referred to the Department of Nuclear Medicine for an ^{18}F-FDOPA PET scan before September 1, 2008.

After approval from the Institutional Review Board was obtained, we included 25 consecutive patients (9 men, 16 women; median age, 51 y; age range, 26–68 y) in a retrospective study. Four patients (patients 10, 12, 13, and 21) had previously undergone resection of pheochromocytomas and were referred for evaluation of recurrence and possible additional sites of involvement (Table 2). All patients underwent standardized whole-body ^{18}F-FDOPA PET or PET/CT studies. ^{18}F-FDOPA was synthesized according to a previously reported procedure (*14,15*).

PET Image Acquisition

Eleven patients underwent ^{18}F-FDOPA whole-body PET studies. PET was performed with an ECAT HR+ system (CTI/

TABLE 2. Cohort Demographic, Clinical, PET, and PET/CT Findings

Patient no.	Age (y)	Sex	Wt (kg)	Modality	SUVmax	Dmax	Location	Biochem Dx	Visual Dx	Final Dx	Histopathology
1	29	M	127	PET				Positive	Negative	Positive	
2	63	F	98	PET					Negative		
3	57	M	84	PET					Negative		
4	43	F	100	PET					Negative		
5	55	F	55	PET					Negative		
6	56	F	70	PET					Negative		
7	61	F	89	PET					Negative		
8	31	M	90	PET	14.59		Left abdomen	Positive	Positive	Positive	Paraganglioma
9	52	M	86	PET	5.41		Right adrenal		Positive	Positive	Pheochromocytoma
10	38	F	73	PET/CT	1.96	13	Right adrenal		Negative	Positive	Pheochromocytoma (malignant)
11	36	F	53	PET					Negative		Normal duodenum
12	49	M	77	PET/CT	2.61	63.1	Right pelvis	Positive	Positive	Positive	Paraganglioma (malignant)
13	55	M	78	PET/CT	2.29	32.7	Thoracic spine	Positive	Positive	Positive	Pheochromocytoma (malignant)
14	53	F	58	PET/CT	11.02	39.7	Left adrenal	Positive	Positive	Positive	Pheochromocytoma
15	52	M	113	PET/CT		38.9	Left adrenal	Negative	Negative		Adrenal cortical adenoma
16	39	M	103	PET/CT		77.5	Left adrenal	Negative	Negative		Castleman disease
17	50	F	82	PET	10		Left adrenal	Positive	Positive	Positive	Pheochromocytoma
18	38	F	58	PET/CT		36.5	Right adrenal	Negative	Negative		Metastatic lung adenocarcinoma
19	58	F	73	PET/CT	28.99	86.9	Right adrenal		Positive	Positive	
20	51	F	88	PET/CT	6.58	69.2	Left adrenal	Positive	Positive	Positive	Pheochromocytoma
21	25	F	57	PET/CT	34.92	46.3	Mediastinum	Positive	Positive	Positive	Paraganglioma
22	43	M	72	PET/CT	22.92	61.9	Right adrenal	Positive	Positive	Positive	Pheochromocytoma
23	46	F	64	PET/CT		44	Right adrenal	Negative	Negative		Adrenal cortical adenoma
24	65	F	93.2	PET/CT		65.2	Left Adrenal	Negative	Negative		Adrenal cortical adenoma
25	68	F	70	PET/CT	4.85	45.9	Left adrenal	Positive	Positive	Positive	Pheochromocytoma

Wt = Weight; Dmax = maximal diameter; Biochem Dx = diagnosis based on biochemistry; Visual Dx = diagnosis based on visual assessment; Final Dx = final diagnosis.

Siemens). The patients were asked to fast for at least 6 h before the examination, to achieve optimal conditions for uptake of the radiopharmaceutical agent. A transmission scan of 3 min/bed position in 2-dimensional mode was acquired first. Subsequently, a median dose of ^{18}F-FDOPA (581 MBq; 4.7–10 MBq/kg; range, 537–625 MBq) was administered intravenously. After a 45-min uptake period, the emission scan was obtained in 3-dimensional mode for 4 min/per bed position. Eight to 10 bed positions with a 58.3-cm transaxial field of view were measured. The images were reconstructed with iterative techniques: maximum a posteriori maximization (*16*) for the transmission scan and ordered-subset expectation maximization consisting of 2 iterations with 8 subsets (*17*) for the emission scan. Corrections for attenuation and scatter were applied. No filtering before or after the scan was used. The final volume set had a transverse matrix size of 128 × 128, resulting in voxel size of 5.1 × 5.1 × 5.1 mm.

PET/CT Image Acquisition

Fourteen patients underwent ^{18}F-FDOPA whole-body PET/CT studies. The patients were asked to fast for at least 6 h before the examination. The last 5 patients received 200 mg of carbidopa 1 h before radiotracer injection to increase the tumor-to-background ratio of tracer uptake. A median dose of ^{18}F-FDOPA (385 MBq; 2–10 MBq/kg; range, 206–577 MBq) was injected. PET/CT was performed with a whole-body PET/CT scanner (Siemens/CTI Reveal). The CT was a dual-slice system. Diagnostic-quality CT images were acquired, with the following parameters: 130 kVp, 120 mA·s, 1-s rotation, 4-mm section collimation, 5-mm section thickness, and 10-mm feed per rotation with a pitch of 1.3 mm/s. CT images were acquired after intravenous injection of iohexol (110–120 mL) (Omnipaque 350; GE Healthcare), except for 1 patient, who underwent recent ^{18}F-FDG PET/CT with intravenous contrast in an outside facility. The PET component was a lutetium oxyorthosilicate detector, 3-dimensional system. After the whole-body CT scan, PET images were obtained 60 min after injection and acquisition time per bed position was 1–5 min, depending on patient body weight, as previously published (*18,19*). Emission scans in patients weighing less than 59 kg were acquired for 1 min/bed position, and scans in those patients weighing more than 91 kg were acquired for 5 min. Images were acquired at multiple bed positions from approximately the patients' middle thighs to the base of the skull. To minimize misregistration, CT and PET were acquired during shallow breathing (*20*). Image reconstruction was performed by using an iterative procedure (ordered-subset expectation maximization, 2 iterations, 8 subsets) and postinjection CT-based photon attenuation correction.

Interpretation of PET and PET/CT Studies

PET and PET/CT images were interpreted by 2 board-certified nuclear medicine physicians using image analysis and fusion software (Mirada; CTI). The interpreters were unaware of the patients' clinical history, laboratory results, and prior imaging studies. The locations of abnormal tracer uptake were recorded, and any visible uptake above normal background was considered abnormal. The sizes of the lesions were measured on PET/CT images by 2 investigators. A 3-dimensional region of interest was manually drawn around areas of abnormal uptake, and the maximum standardized uptake value (SUVmax) was determined. Images were interpreted as positive or negative for pheochromocytoma or paraganglioma by consensus.

Histopathology

The gold standard for the diagnosis of pheochromocytoma is histopathologic evaluation of 4-μm-thick, hematoxylin- and eosin-stained sections prepared from representative, paraffin-embedded tissue sections of surgical specimens after fixation in 10% buffered formalin. Confirmatory immunohistochemical staining is performed using standard procedures in a DAKO autostainer using antisera against S-100 (1:500; DAKO), chromogranin (1:1,000; DAKO), and synaptophysin (1:100; DAKO). Pheochromocytomas exhibit positivity for chromogranin and synaptophysin. In addition, S-100 immunostain highlights the presence of sustentacular cells that typically surround nests of tumor cells.

Composite Reference

Because histologic verification, which would have been the most accurate reference standard, was not feasible in all cases, a combination of follow-up evaluations, laboratory findings, and other imaging modalities was used as the reference standard to determine the accuracy of ^{18}F-FDOPA PET and PET/CT in the diagnosis of pheochromocytoma.

Statistics

The Fisher exact test was used to compare the number of true and false findings in ^{18}F-FDOPA PET and PET/CT studies. Sensitivity, specificity, and accuracy of combined data were calculated using the composite reference standard. For correlations between SUVmax of the ^{18}F-FDOPA uptake in the tumors and biochemical parameters, the Spearman nonparametric correlation coefficient was calculated. The SUVmax of benign and malignant tumors was compared using the Mann–Whitney nonparametric analysis. A 2-sided P value of less than 0.05 was considered significant.

RESULTS

Eleven patients underwent ^{18}F-FDOPA PET studies, and 14 patients underwent ^{18}F-FDOPA PET/CT studies. The examiners, who were unaware of the clinical findings and laboratory results, detected and localized lesions with abnormally elevated tracer activity in 3 PET and 8 PET/CT studies (Table 2; Figs. 1–5). These lesions had an SUVmax ranging from 2.3 to 34.9 (median, 10), and the maximum diameter of the lesions ranged from 33 to 87 mm (median, 55 mm) for the PET/CT studies.

A subsequent review of the studies revealed 2 false-negatives cases. A positive lesion measuring 13 × 5 mm with an SUVmax of 1.96 was detected in the right adrenal bed, adjacent to the liver in 1 patient (patient 10, Fig. 1), but had not been detected in the visual evaluation. This patient had undergone surgical resection previously. This case was considered false-negative in the analysis. In another patient with typical clinical findings and strongly positive biochemical markers (patient 1), multiple imaging studies including PET, CT, MRI, and metaiodobenzylguanidine (MIBG) did not visualize any lesion. Because of the lack of tumor localization, this patient did not undergo surgery. Subsequent ^{131}I-MIBG therapy led to some improvement in symptoms, and the case was considered false-negative for pheochromocytoma.

One of the patients (patient 19, Fig. 2) with positive biochemical and PET/CT findings had extensive retroper-

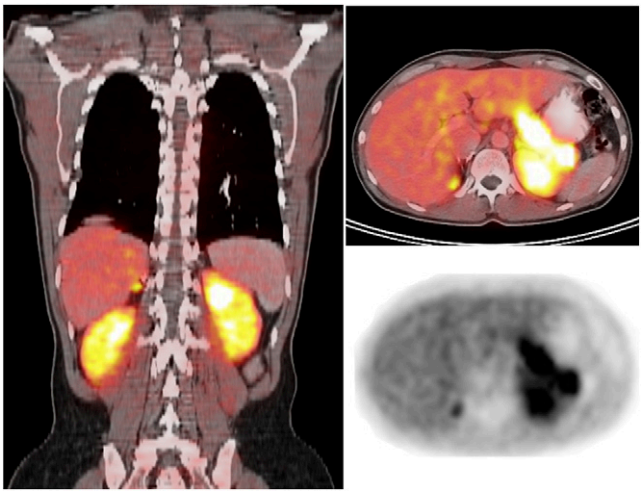

FIGURE 1. Residual or recurrent pheochromocytoma in right adrenal bed (patient 10).

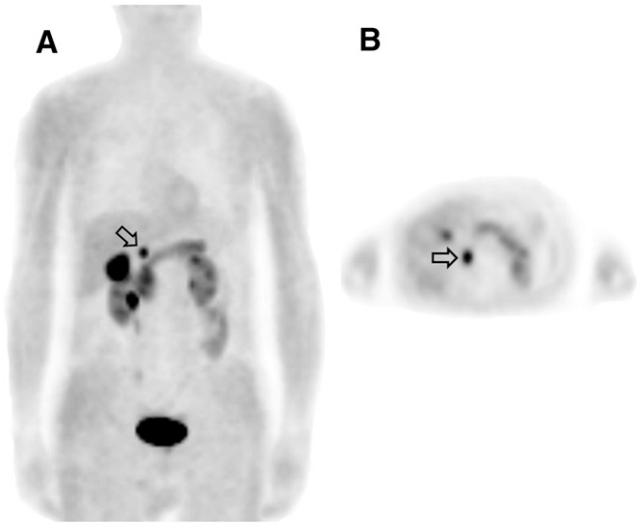

FIGURE 3. Right adrenal pheochromocytoma (patient 9). (A) Anterior view of maximum-intensity-projection image demonstrates right adrenal pheochromocytoma (open arrow) and adjacent pancreas, gallbladder, kidneys, and liver. (B) Transverse cross-section through tumor.

itoneal involvement along the sympathetic chain extending into the caudate lobe of the liver and engulfing the inferior vena cava. This tumor was deemed unresectable by the tumor board. This case was considered true-positive without histologic confirmation.

Seventeen of the 25 patients (68%) underwent surgery. Histologic evaluation of the lesions revealed pheochromocytoma and paraganglioma in 11 cases (44%) (patients 8–10, 12–14, 17, 20–22, and 25; Figs. 3 and 4), nonchromaffin cell tumors in 5 cases, adrenal cortical adenomas in 3 cases (12%) (patients 15, 23, and 24; Fig. 5), Castleman disease in 1 case (patient 16), metastatic mucinous adenocarcinoma of lung primary in 1 case (patient 18), and normal duodenal tissue in 1 case (patient 11) (Table 2). The remaining patients had a minimum of 4 y of clinical follow-up.

Statistical analysis of the visual interpretation of PET and PET/CT studies using the Fisher exact test did not show statistically significant differences between the 2 modalities ($P = 1$). Therefore, further analysis was performed on combined data. The sensitivity of ^{18}F-FDOPA PET and PET/CT studies for diagnosis of chromaffin cell tumors was 84.6% (95% confidence interval, 53.7%−97.3%) on the basis of findings in the 11 histologically confirmed cases and 2 false-negative cases (patients 1 and 10). Because there was no false-positive finding, the specificity was 100% (95% confidence interval, 69.9%−100%) (Table 3).

Biochemical work-up of 15 patients was available for this study. Ten patients (67%) had significantly elevated biochemical markers that were diagnostic of pheochromo-

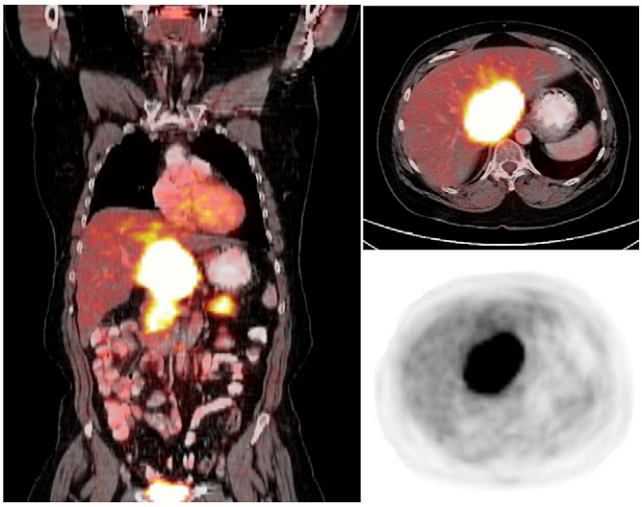

FIGURE 2. Unresectable pheochromocytoma (patient 19).

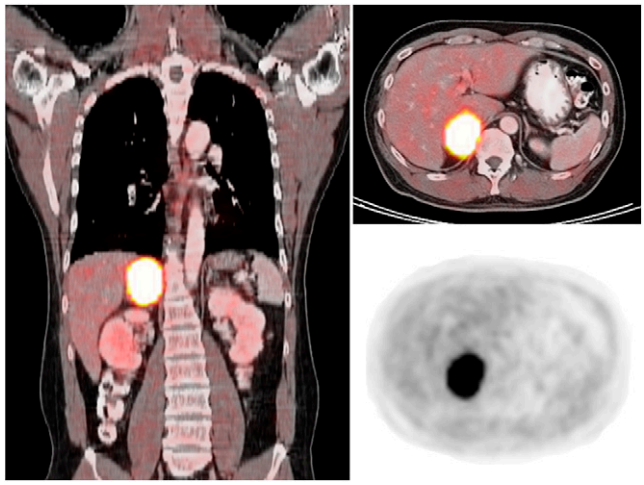

FIGURE 4. Right adrenal pheochromocytoma (patient 22).

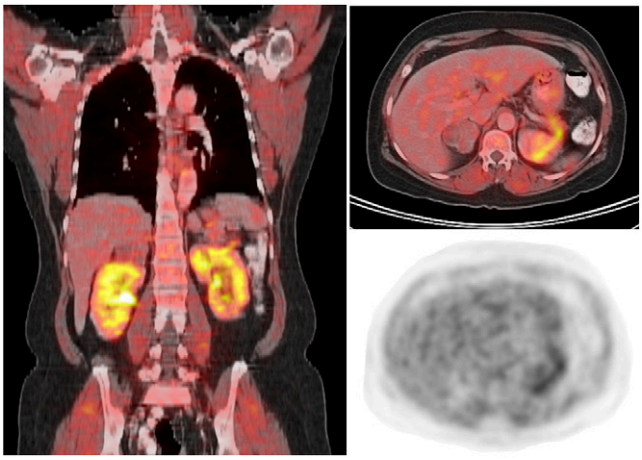

FIGURE 5. Right adrenal cortical adenoma (patient 23).

TABLE 4. Correlation Between SUVmax and Levels of Plasma Biochemicals

Patient no.	SUVmax	NE	MN	NMN	Ch
8	14.59		1.24	14.3	171
9	5.41	911	0.43	2.69	23.6
12	2.61	4,869	<0.2	39.2	
13	2.29		0.2	6.95	136
14	11.02	1,434	0.06	3.72	
17	10.00		1.59	5.42	
20	6.58				337
22	22.92	5,800	0.29	21.5	123.4
25	4.85		15	1.14	
Spearman ρ		0.4	0.19	0.143	0.1
P		0.6	0.651	0.736	0.873

NE = norepinephrine (pg/mL); MN = metanephrine (nmol/L); NMN = normetanephrine (nmol/L); Ch = chromogranin (ng/mL).

cytoma (*21,22*). Genetic analysis was performed on 4 patients, revealing a succinate dehydrogenase complex subunit B mutation for patients 13 and 21, von Hippel-Lindau mutation for patient 14, and no detectable genetic abnormality for patient 12. To evaluate whether uptake of ^{18}F-FDOPA in pheochromocytoma lesions is independent of plasma or urinary biochemical levels, correlation between SUVmax of the lesions and biochemical levels was analyzed. Spearman nonparametric analysis did not demonstrate a statistically significant correlation, at the 0.05 level, between SUVmax of the tumors and plasma or urinary biochemical measurements (Tables 4 and 5). This lack of correlation confirms that the SUVmax of the tumors represents an independent indicator of presence of disease.

Three patients (patients 10, 12, and 13) were diagnosed with malignant pheochromocytomas. Malignant pheochromocytomas were defined as tumors presenting either initially or subsequently with foci outside known chromaffin sites. All 3 patients had undergone surgical resection of the primary lesions before this study. Although the metastatic lesions, compared with the benign tumors, detected on the initial ^{18}F-FDOPA PET/CT examinations of all 3 patients demonstrated relatively low ^{18}F-FDOPA uptake, a subsequent ^{18}F-FDOPA PET/CT study of 1 of the patients (patient 10) revealed multiple foci of intense ^{18}F-FDOPA uptake (SUVmax, 16.6) consistent with widespread metastatic disease. Statistical analysis using the Mann–Whitney nonparametric test did not demonstrate a statistically significant difference in SUVmax between malignant and benign tumors.

TABLE 3. Summary of Visual Analysis

Parameter	PET	PET/CT	Combined
TP	3	8	11
TN	7	5	12
FP	0	0	0
FN	1	1	2
Total	11	14	25
Sensitivity	75.0%	88.9%	84.6%
Specificity	100.0%	100.0%	100.0%
PPV	100.0%	100.0%	100.0%
NPV	87.5%	83.3%	85.7%

TP = true-positive; TN = true-negative; FP = false-positive; FN = false-negative; PPV = positive predictive value; NPV = negative predictive value.

DISCUSSION

This study demonstrated no false-positive findings. Two false-negative cases were identified. One patient underwent a PET/CT study that was performed after surgery for evaluation of recurrence. Review of this case revealed that a 13 × 5 mm lesion with an SUVmax of 1.96 in the right adrenal bed had been missed on the initial visual analysis. The second false-negative finding occurred in a patient with typical clinical manifestations who had the highest levels of biochemical markers in our study group. Evaluation of this patient with several imaging modalities did not detect any lesion. However, subsequent treatment of this patient with ^{131}I-MIBG led to partial improvement of symptoms. Failure in detection of the tumor could be secondary to several factors, including the small size of the lesion; location of the tumor in or near organs with high physiologic ^{18}F-FDOPA activity such as the pancreas, biliary and urinary systems; or true loss of ^{18}F-FDOPA uptake due to a general process of dedifferentiation as it has been recognized in ^{123}I-MIBG uptake (*23*).

This study demonstrates multiple advantages of ^{18}F-FDOPA PET and PET/CT in preoperative localization of lesions and confirmation of diagnosis in suspected cases of pheochromocytoma. Catecholamine-based testing can be confounded by several medications that are known to yield false-positive results (*24*). Often patients are unable to stop taking these medications (e.g., psychotropic medications), and for the patients, the only biochemical test available is chromogranin A, which is neither sensitive nor specific.

TABLE 5. Correlation Between SUVmax and Levels of Urinary Biochemicals

Patient no.	SUVmax	NE	E	D	Total MN	MN	NMN	VMA
1	1	3,380	389	69,548	3,490			102.2
8	14.59	345	19	326	4,903	652	4,251	25.8
12	2.61	1,220	5.9	74	17,994	155	17,839	
13	2.29	216		153	3,549	20	3,549	
14	11.02	138	2.8	242	2,855	111	2,744	12
17	10.00	90	29	945	3,456	1,302	2,154	9.3
20	6.58	368	325	801	12,711	8,294	4,417	
21	34.92	978		607	4,175	108	4,067	13.6
22	22.92	1,068	9.1	215	5,680	111	5,569	21.1
25	4.85	46	317	320	15,487	14,783	704	
Spearman ρ		−0.103	−0.5	0.018	−0.067	−0.184	0.117	−0.086
P		0.777	0.207	0.96	0.855	0.635	0.765	0.872

NE = norepinephrine (μg/24 h); E = epinephrine (μg/24 h); D = dopamine (μg/24 h); MN = metanephrine (μg/24 h); NMN = normetanephrine (μg/24 h); VMA = vanyl mandelic acid (mg/24 h).

^{18}F-FDOPA PET/CT eliminates this conundrum and diagnoses these patients without a need for the patients to discontinue their medications. The patients with borderline elevated catecholamines constitute another diagnostic challenge. Some investigators have recommended clonidine suppression testing (*25*), but this is labor-intensive and would require personnel training to be performed accurately. Our data show that ^{18}F-FDOPA PET is a reliable functional imaging modality that can be used as part of the diagnostic work-up in cases in which all previous tests did not lead to a definite diagnosis, without the need for clonidine suppression testing. In the appropriate clinical context, ^{18}F-FDOPA PET can confirm or reject the diagnosis of pheochromocytoma. This ability of ^{18}F-FDOPA PET carries major clinical impact on presurgical preparation of the patients and surgical planning.

Nonparametric statistical analysis of our data using the Spearman correlation coefficient test demonstrated that the SUVmax of the tumors did not have a statistically significant correlation with biochemical assays in positive cases. This result can be explained by complex pathways and kinetics of the biochemical processes. SUVmax represents tumoral radiopharmaceutical accumulation, which depends on the uptake rate of ^{18}F-FDOPA, biochemical reactions, and the rate of active or passive release of biochemical products. Plasma levels of biochemical components and 24-h urinary levels are mainly secondary to the rate of production, release, and clearance. This characteristic implies that ^{18}F-FDOPA PET can be used for diagnosis of suspected cases, independent of plasma and urinary catecholamine levels.

PET with ^{18}F-FDOPA is based on the ability of neuroendocrine tumors to take up, decarboxylate, and store amino acids, such as DOPA (*26–28*). The special advantage of ^{18}F-FDOPA PET, compared with conventional scintigraphic methods, is the lack of accumulation of ^{18}F-FDOPA in the normal adrenal glands, which may occur in as many as 32%−75% of patients 24 h after administration of ^{131}I-MIBG (*29,30*). Furthermore, the higher spatial resolution of PET enables detection of small lesions and metastatic lymphadenopathies. PET can be performed shortly after the administration of ^{18}F-FDOPA, as opposed to waiting the 24–48 h necessary for ^{131}I-MIBG scanning, and provides tomographic images instead of planar images. The selective tracer accumulation in the target cells, low background uptake—in combination with higher resolution—and 3-dimensional acquisition yield excellent-quality whole-body images that significantly improve image interpretation. In addition, discontinuation of medications is not necessary for ^{18}F-FDOPA PET. Interference of medications with ^{18}F-FDOPA uptake, which is a well-known phenomenon in MIBG imaging, has not been reported. In our study, all PET and PET/CT studies were performed while the patients continued their medications without interruption. Another advantage of ^{18}F-FDOPA PET is less radiation exposure (*31,32*); in conventional ^{131}I-MIBG, radiation exposure necessitates thyroid blocking with administration of iodine.

This study has several limitations. Because of the low prevalence of the disease, we included only 3 patients with metastatic pheochromocytoma. Thus, future studies are needed to investigate the value of ^{18}F-FDOPA PET in patients with metastatic disease. Second, the whole-body biodistribution of ^{18}F-FDOPA with relatively high uptake in the pancreas, biliary and urinary systems could induce image misinterpretations. For instance, normal pancreatic tracer activity might spill over or project onto the region of the adrenals, causing a false-positive interpretation. Conversely, abnormal adrenal uptake might be masked by physiologic background activity, causing false-negative scan interpretations. However, combined PET/CT can probably reduce or even eliminate this source of error. Third, 1 study has reported that medication in advance with carbidopa may increase tumor uptake of ^{18}F-FDOPA (*11*). However, this study reported a moderate increase in sensitivity with the addition of carbidopa from 55.6% to

66.7%. Finally, the current study did not attempt a comparison with other probes such as amino acid analogs or MIBG that could be used for imaging of neuroendocrine tumors. Therefore, it remains unknown whether ^{18}F-FDOPA is equivalent or superior to these other approaches.

CONCLUSION

On the basis of these results, ^{18}F-FDOPA PET and PET/CT are valuable tools not only for improving detectability but also for precisely localizing the tumors, especially when they arise from the adrenal glands.

ACKNOWLEDGMENT

Financial support was received from the Department of Molecular and Medical Pharmacology, UCLA, Los Angeles, California.

REFERENCES

1. Ilias I, Pacak K. Current approaches and recommended algorithm for the diagnostic localization of pheochromocytoma. *J Clin Endocrinol Metab.* 2004; 89:479–491.
2. Martiniova L, Ohta S, Guion P, et al. Anatomical and functional imaging of tumors in animal models: focus on pheochromocytoma. *Ann N Y Acad Sci.* 2006;1073:392–404.
3. Brink I, Hoegerle S, Klisch J, Bley TA. Imaging of pheochromocytoma and paraganglioma. *Fam Cancer.* 2005;4:61–68.
4. Mann GN, Link JM, Pham P, et al. [^{11}C]metahydroxyephedrine and [^{18}F]fluorodeoxyglucose positron emission tomography improve clinical decision making in suspected pheochromocytoma. *Ann Surg Oncol.* 2006;13:187–197.
5. Shulkin BL, Wieland DM, Schwaiger M, et al. PET scanning with hydroxyephedrine: an approach to the localization of pheochromocytoma. *J Nucl Med.* 1992;33:1125–1131.
6. Trampal C, Engler H, Juhlin C, Bergström M, Långström B. Pheochromocytomas: detection with ^{11}C hydroxyephedrine PET. *Radiology.* 2004;230:423–428.
7. Ilias I, Chen CC, Carrasquillo JA, et al. Comparison of 6-^{18}F-fluorodopamine PET with ^{123}I-metaiodobenzylguanidine and ^{111}In-pentetreotide scintigraphy in localization of nonmetastatic and metastatic pheochromocytoma. *J Nucl Med.* 2008;49:1613–1619.
8. Timmers HJ, Carrasquillo JA, Whatley M, et al. Usefulness of standardized uptake values for distinguishing adrenal glands with pheochromocytoma from normal adrenal glands by use of 6-^{18}F-fluorodopamine PET. *J Nucl Med.* 2007;48:1940–1944.
9. Kaji P, Carrasquillo JA, Linehan WM, et al. The role of 6-[^{18}F]fluorodopamine positron emission tomography in the localization of adrenal pheochromocytoma associated with von Hippel-Lindau syndrome. *Eur J Endocrinol.* 2007;156:483–487.
10. Hoegerle S, Nitzsche E, Altehoefer C, et al. Pheochromocytomas: detection with ^{18}F DOPA whole body PET—initial results. *Radiology.* 2002;222:507–512.
11. Timmers HJ, Hadi M, Carrasquillo JA, et al. The effects of carbidopa on uptake of 6-^{18}F-fluoro-L-DOPA in PET of pheochromocytoma and extraadrenal abdominal paraganglioma. *J Nucl Med.* 2007;48:1599–1606.
12. Taieb D, Tessonnier L, Sebag F, et al. The role of ^{18}F-FDOPA and ^{18}F-FDG-PET in the management of malignant and multifocal pheochromocytomas. *Clin Endocrinol.* 2008;69:580–586.
13. Brink I, Schaefer O, Walz M, Neumann HP. Fluorine-18 DOPA PET imaging of paraganglioma syndrome. *Clin Nucl Med.* 2006;31:39–41.
14. Bishop A, Satyamurthy N, Bida G, Hendry G, Phelps M, Barrio JR. Proton irradiation of [^{18}O]O_2: production of [^{18}F]F2 and [^{18}F]F2 + [^{18}F] OF2. *Nucl Med Biol.* 1996;23:189–199.
15. Namavari M, Bishop A, Satyamurthy N, Bida G, Barrio JR. Regioselective radiofluorodestannylation with [^{18}F]F2 and [^{18}F]CH3COOF: a high yield synthesis of 6-[^{18}F]fluoro-L-dopa. *Int J Rad Appl Instrum [A].* 1992;43:989–996.
16. Nuyts J, Baete K, Bequé D, Dupont P. Comparison between MAP and postprocessed ML for image reconstruction in emission tomography when anatomical knowledge is available. *IEEE Trans Med Imaging.* 2005;24:667–675.
17. Nuyts J, Michel C, Dupont P. Maximum-likelihood expectation-maximization reconstruction of sinograms with arbitrary noise distribution using NEC-transformations. *IEEE Trans Med Imaging.* 2001;20:365–375.
18. Halpern BS, Dahlbom M, Auerbach MA, et al. Optimizing imaging protocols for overweight and obese patients: a lutetium orthosilicate PET/CT study. *J Nucl Med.* 2005;46:603–607.
19. Halpern BS, Dahlbom M, Quon A, et al. Impact of patient weight and emission scan duration on PET/CT image quality and lesion detectability. *J Nucl Med.* 2004;45:797–801.
20. Allen-Auerbach M, Yeom K, Park J, Phelps M, Czernin J. Standard PET/CT of the chest during shallow breathing is inadequate for comprehensive staging of lung cancer. *J Nucl Med.* 2006;47:298–301.
21. Kudva YC, Sawka AM, Young WF Jr. Clinical review 164: the laboratory diagnosis of adrenal pheochromocytoma—the Mayo Clinic experience. *J Clin Endocrinol Metab.* 2003;88:4533–4539.
22. Pacak K, Eisenhofer G, Ahlman H, et al. Pheochromocytoma: recommendations for clinical practice from the First International Symposium. October 2005. *Nat Clin Pract Endocrinol Metab.* 2007;3:92–102.
23. van der Harst E, de Herder WW, Bruining HA, et al. [^{123}I]metaiodobenzylguanidine and [^{111}In]octreotide uptake in benign and malignant pheochromocytomas. *J Clin Endocrinol Metab.* 2001;86:685–693.
24. Harding JL, Yeh MW, Robinson BG, Delbridge LW, Sidhu SB. Potential pitfalls in the diagnosis of phaeochromocytoma. *Med J Aust.* 2005;182:637–640.
25. Eisenhofer G, Goldstein DS, Walther MM, et al. Biochemical diagnosis of pheochromocytoma: how to distinguish true- from false-positive test results. *J Clin Endocrinol Metab.* 2003;88:2656–2666.
26. Uchino H, Kanai Y, Kim DK, et al. Transport of amino acid-related compounds mediated by L-type amino acid transporter 1 (LAT1): insights into the mechanisms of substrate recognition. *Mol Pharmacol.* 2002;61:729–737.
27. Pearse AG. The cytochemistry and ultrastructure of polypeptide hormone-producing cells of the APUD series and the embryologic, physiologic and pathologic implications of the concept. *J Histochem Cytochem.* 1969;17:303–313.
28. Bergstrom M, Eriksson B, Oberg K, et al. In vivo demonstration of enzyme activity in endocrine pancreatic tumors: decarboxylation of carbon-11-DOPA to carbon-11-dopamine. *J Nucl Med.* 1996;37:32–37.
29. Lynn MD, Shapiro B, Sisson JC, et al. Portrayal of pheochromocytoma and normal human adrenal medulla by m-[^{123}I]iodobenzylguanidine: concise communication. *J Nucl Med.* 1984;25:436–440.
30. Elgazzar AH, Gelfand MJ, Washburn LC, et al. I-123 MIBG scintigraphy in adults: a report of clinical experience. *Clin Nucl Med.* 1995;20:147–152.
31. Wafelman AR, Suchi R, Hoefnagel CA, Beijnen JH. Radiochemical purity of iodine-131 labelled metaiodobenzylguanidine infusion fluids: a report from clinical practice. *Eur J Nucl Med.* 1993;20:614–616.
32. Brown WD, Oakes TR, DeJesus OT, et al. Fluorine-18-fluoro-L-DOPA dosimetry with carbidopa pretreatment. *J Nucl Med.* 1998;39:1884–1891.